INTERNATIONAL JOURNAL OF RESEARCH SCIENCE & MANAGEMENT

TIME FREQUENCY TRAINING ESTIMATION METHOD OF OFDM FOR MOBILE LARGE SCALE MIMO SYSTEMS

CH.Hasini [1*], P.Ratna Bhaskar[2]
[1*]SRK Institute of Technology, PG Scholar
[2]SRK Institute of Technology, Assistant Professor
*Correspondence Author: cherukupallihasini@gmail.com

Keywords: large-scale MIMO, OFDM, spectral efficiency, time-frequency training (TFT), time frequency joint channel estimation.

Abstract
This overview portrays the 40 year evolution of orthogonal frequency division multiplexing (OFDM) research. the amelioration of powerful multicarrier OFDM arrangements with multiple- input multiple output(MIMO) systems has numerous benefits, this paper, we propose time frequency training OFDM(TFT OFDM) transmission scheme for large scale MIMO systems, where each TFT-OFDM symbol without cyclic prefix adopts the time-domain training sequence (TS) and the frequency-domain orthogonal grouped pilots as the time frequency training information We also derive the theoretical Cramer-Rao lower bound (CRLB) of the proposed channel estimator. Compared with conventional large-scale OFDM MIMO systems, we can also implement the MMSE method to improve the spectral efficiency.

Introduction
Due to the robustness to the frequency-selective multipath channel and the low complexity of the frequency domain equalizer, orthogonal frequency division multiplexing (OFDM) has been widely recognized as one of the key techniques for the next generation broadband wireless communication (BWC) systems [2]. One fundamental issue of OFDM is the block transmission scheme. Basically, there are three types of OFDM-based block transmission schemes: cyclic prefix OFDM (CP-OFDM) [3], zero padding OFDM (ZP-OFDM) [4], and time domain synchronous OFDM (TDS-OFDM) [4]. The broadly used CPOFDM scheme utilizes the CP to eliminate the inter-block interference (IBI) as well as the inter-carrier-interference (ICI) [6]. However, the main drawback of TDS-OFDM is that, the time-domain TS and the OFDM data block will cause IBI to each other. Thus, the iterative interference cancellation algorithm has to be used for channel estimation and equalization [7], [8], One exciting solution to the interference problem of TDS-OFDM is the cyclic postfix OFDM scheme [9], [10], in this paper the spectrally efficient time-frequency training OFDM (TFTOFDM) transmission scheme for large-scale MIMO systems. The rest of this paper is organized as follows. The system model of the proposed TFT-OFDM MIMO scheme and the preamble-based channel estimators in both the time and frequency domains are discussed in Section II. Addresses the channel tracking and data detection for TFT-OFDM MIMO systems. The performance analysis of the proposed scheme is provided in Section III before simulation results are presented in Section IV. Finally, conclusions are drawn in Section V

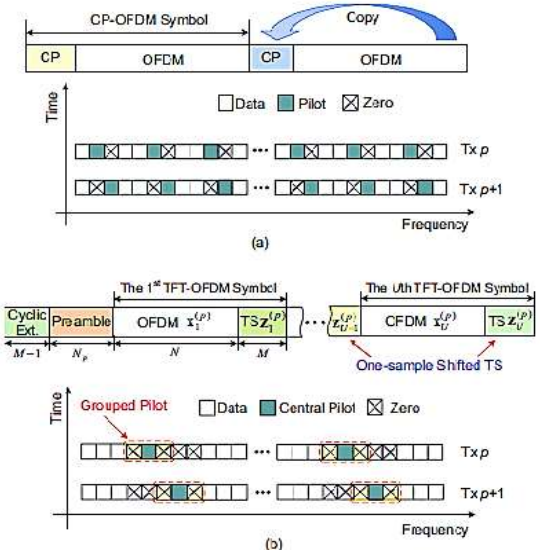

INTERNATIONAL JOURNAL OF RESEARCH SCIENCE & MANAGEMENT

Fig.1. Time-frequency signal structure comparison: a) CP-OFDM MIMO with frequency-domain training information (pilots) only; b) The proposed TFT-OFDM MIMO with both time- and frequency-domain training information for every OFDM data block

Tft-ofdm system model

In this section, the time-frequency signal structure of the proposed TFT-OFDM MIMO scheme is described at first, and then the system model is presented.

Time-frequency signal structure of tft-ofdm

Fig. 1 compares the time-frequency signal structure of CPOFDM MIMO and the proposed TFT-OFDM MIMO. As shown in Fig. 1 (b), the TFT-OFDM signals are transmitted frame by frame, whereby each frame is composed of one preamble with its cyclic extension and the following *U* TFTOFDM symbols (sub frames).We assume N_t transmit antennas and N_r receive antennas in MIMO systems. In the time domain, unlike CP-OFDM where the CP is utilized as the guard interval, the *i*th TFT-OFDM symbol $S_i^{(p)}$ $(1 \le i \le U)$ for the *p*th transmit antenna $(1 \le p \le N_t)$ is composed of the length-*N* OFDM symbol $x_i^{(p)} = [x_{i,0}^{(p)}, x_{i,1}^{(p)}, \ldots x_{i,N-1}^{(p)}]^T$ and the followed length-*M*

TS $\mathbf{z}_i^{(p)} = [z_{i,0}^{(p)}, z_{i,1}^{(p)}, \cdots, z_{i,M-1}^{(p)}]^T$ as below

$$\mathbf{s}_i^{(p)} = \begin{bmatrix} \mathbf{x}_i^{(p)} \\ \mathbf{z}_i^{(p)} \end{bmatrix}_{(N+M)\times 1} = \begin{bmatrix} \mathbf{F}_N^H \mathbf{X}_i^{(p)} \\ \mathbf{z}_i^{(p)} \end{bmatrix}_{(N+M)\times 1}, \quad (1)$$

Where $X_i^{(p)} = F_N X_i^{(p)}$. Since it has been proved in [1]. In the frequency domain, TFT-OFDM MIMO systems adopts *G* orthogonal pilot groups randomly scattered within the signal bandwidth, where each pilot group has only one non-zero central pilot in the middle surrounded by *d* zero pilots on the left and right sides (in Fig. 1 (b), *d* = 1 is used as an example). Although frequency-domain pilots are common in OFDM systems, the proposed pilot pattern has the following four distinct features. [1].

System model of tft-ofdm mimo

In MIMO systems, for a certain receive antenna, the Channel impulse response (CIR) $h_i^{(p)}$ associated with the *p*th transmit antenna during the *i*th TFT-OFDM symbol can be denoted by

$$h_i^{(p)} = [h_{i,0}^{(p)}, h_{i,1}^{(p)}, \ldots., h_{i,L-1}^{(p)}]^T \qquad (2)$$

Where $h_{i,l}^{(p)}$ *i*s the path gain of the *l*th path with the path delay $\tau_l^{(p)}$, *L* denotes the maximum channel spread, and *L* = *M* is assumed to avoid the interference between two neighboring OFDM data blocks, so we have $N_p = N_t M = N_t L$. Note that although the delay spread *L* maybe large in frequency selective channels, the number of most significant taps (or resolvable paths) *Q* is usually much smaller than the channel length *L*, i.e., *Q* <<*L*, because of the sparse nature of wireless channels, especially for wideband communications.[1]. For example, the ITU

Vehicular B channel [1] with the maximum delay spread of 20 μs, which is equivalent to *L* = 200 samples at the system sampling rate of 10 MHz, has only *Q* = 6 resolvable paths. Furthermore, it has been proved that the path delays $\{\tau_l^{(p)}\}_{l=0}^{L-1}$ vary much slower than path gains $\{h_{i,l}^{(p)}\}_{l=0}^{L-1}$ (including phases and amplitudes) [1] which is caused by the fact that the duration for the delay of a path to change by one tap is inversely proportional to the signal bandwidth *B*, while the coherence time of the path gains is inversely proportional to the carrier frequency f_c . Since *B* << f_c for almost all of practical wireless systems, path delays would change much slower than path gains. At the receiver, the signals coming from different transmit antennas will mix together, and the received OFDM data block $y_i = [y_{i,0}, y_{i,1,\ldots..}, y_{i,N-1}]^T$ after cyclist reconstruction [1] is

$$y_i = \sum_{p=1}^{N_t} x_i^{(p)} \otimes h_i^{(p)} + w_0 \qquad (3)$$

INTERNATIONAL JOURNAL OF RESEARCH SCIENCE & MANAGEMENT

Where $W_i = [w_{i,0}, w_{i,1,.....,} w_{i,N-1}]^T$ denotes the additive white Gaussian noise (AWGN) vector with zero mean and the variance of $\sigma^2 I_N$. Applying DFT to y_i above, the received signal $y_{i.k}$ on the *k*th subcarrier could be presented by

$$Y_{i,k} = \sum_{p=1}^{N_t} X_{i,k}^{(p)} + W_{i,k}^{(p)} + W_{i,k} \, 0 \le k \le N-1 \quad (4)$$

Where $H_i^{(p)} = [\mathrm{H}_{i,0}^{(p)}, \mathrm{H}_{i,1}^{(p)}, ...H_{i,N-1}^{(p)}]^T$ is the channel frequency response (CFR) of $h_i^{(p)}$, and we have

$$H_i^{(p)} = \sqrt{N} F_{N,L} h_i^{(p)} \quad (5)$$

Where $F_{N,L}$ of size $N \times L$ denotes the first L columns of the DFT matrix **F***N*. In addition, we use $H_0^{(P)}$ and $h_0^{(p)}$ to denote the CFR and CIR during the preamble, respectively.

Preamble based channel estimation:

Based on the preamble of the TFT-OFDM transmission frame, the initial channel estimation can be achieved either in the time or frequency domain. Their equivalence will be also proved in this section.

Time-domain channel estimation:

The received preamble $d_0 = [d_{0,0}, d_{0,1}, ...\mathrm{d}_{(0,\mathrm{N}_{P-1}}]^T$ in the time domain at the receive antenna is immune from the inter-block-interference (IBI) due to the protection of the cyclic extension, so d_0 can be expressed by

$$\mathbf{d}_0 = \sum_{p=1}^{N_t} \mathbf{c}^{(p)} \otimes \mathbf{h}_0^{(p)} + \mathbf{v}_0 = \sum_{p=1}^{N_t} \mathbf{c}_0^{(p)} \mathbf{h}_0^{(p)} + \mathbf{v}_0 = \mathbf{c}_0 \mathbf{h}_0 + \mathbf{v}_0, \quad (6)$$

In (6), there are $N_t L$ unknown parameters in h_0 and N_p observations in d_0. If $N_p \ge N_t L$, the time-domain channel estimate $h_0^{\wedge}$ can be obtained by [11]

$$h_0^{\wedge} = c_0^{+} d_0 = (c_0^H c_0)^{-1} c_0^H d_0 \quad (7)$$

We have $E\{h_0^{\wedge} - h_0\} = E\{(c_0^H c_0)^{-1} c_0^H v_0 = 0_{N_t L * 1}$ due to every element of v_0 has zero mean, so the mean square error (MSE) of the unbiased channel estimator (7) is

$$\begin{aligned} \mathrm{MSE} &= \mathrm{E}\left\{ \left(\widehat{\mathbf{h}}_0 - \mathbf{h}_0\right)^H \left(\widehat{\mathbf{h}}_0 - \mathbf{h}_0\right) \right\} \\ &= \mathrm{tr}\left\{ \left(\mathbf{c}_0^H \mathbf{c}_0\right)^{-1} \mathbf{c}_0^H \mathrm{E}\left\{ \mathbf{v}_0 \mathbf{v}_0{}^H \right\} \mathbf{c}_0 \left(\mathbf{c}_0^H \mathbf{c}_0\right)^{-1} \right\} \\ &= \sigma^2 \mathrm{tr}\left\{ \left(\mathbf{c}_0^H \mathbf{c}_0\right)^{-1} \right\}. \end{aligned} \quad (8)$$

According to the proof in the Appendix[1], the minimum MSE can be achieved by the following optimal design criterion

$$\mathbf{c}_0^H \mathbf{c}_0 = N_t L \mathbf{I}_{N_t L}. \quad (9)$$

The corresponding MSE in (8) is then derived as

$$\mathrm{MSE}_{\min} = \sigma^2 \mathrm{tr}\left\{ \frac{1}{N_t L} \mathbf{I}_{N_t L} \right\} = \sigma^2. \quad (10)$$

INTERNATIONAL JOURNAL OF RESEARCH SCIENCE & MANAGEMENT

Thus, the minimum MSE (10) can be achieved, and the time-domain channel estimator (7) is then simplified by circular correlation [1] as

$$\widehat{\mathbf{h}}_0 = \frac{1}{N_t L}\mathbf{c}_0^H \mathbf{d}_0 = \frac{1}{N_t L}\mathbf{c} \otimes \mathbf{d}_0. \quad (11)$$

Frequency-domain channel estimation:

The frequency-domain signal model (4) is also valid when N_p-point DFT instead of *N*-point DFT is used to produce the received preamble $D_0 = [D_{0,0}, D_{0,1}, ...D_0, N_{p-1}]^T$ in the frequency domain, i.e.,

$$D_0 = C_0 H_0 + V_0 \quad (12)$$

Where $V_0 = F_{N_P} v_0$ denotes AWGN, $D_0 = F_{N_P} d_0$ presents the N_p-point DFT of the time-domain received preamble d_0, $C_0 = [diag\{C^{(1)}\}, diag\{C^{(2)}\}, ..., diag\{C^{N_t}\}] d_0$ denotes the $N_p \times N_t$ N_p frequency-domain training matrix based on $\{C^{(p)}\}_{p=1}^{N_t}$, and the CFR H_0 during the preamble can be related to the corresponding CIR h_0 by using (5) as

$H_0 = F_0 h_0$, where

$$\mathbf{F}_0 = \begin{bmatrix} \mathbf{F}_{N_p,L} & \cdots & \mathbf{0}_{N_p \times L} \\ \vdots & \ddots & \vdots \\ \mathbf{0}_{N_p \times L} & \cdots & \mathbf{F}_{N_p,L} \end{bmatrix}_{N_t N_p \times N_t L}. \quad (13)$$

Since there are N_t N_p unknown parameters in H_0 and only N_p observations in D_0, eq. (12) is an underdetermined problem without unique solution. However, this problem can be solved by using the relationship between the CFR H_0 and the CIR h_0 as below

$$D_0 = C_0 F_0 h_0 + V_0 = A_0 h_0 + V_0 \quad (14)$$

Where $A_0 = C_0 F_0$ and the number of unknown parameters is reduced from N_t N_p in (12) to $N_t L$in (14). If $N_p \geq N_t L$, the channel estimation can be achieved by [1]

$$h_0^{\wedge} = A_0^{+} D_0 = ((C_0 F_0)^H C_0 F_0)^{-1} (C_0 F_0)^H D_0 \quad (15)$$

Then, the CFR can be obtained by $H_0^{\wedge} = F_0 h_0^{\wedge} = F_0 A_0^{+} D_0$

Unification of the time- and frequency-domain channel estimators:

The time-domain channel estimator (7) is based on time domain signals d_0 and c_0, while the frequency-domain channel estimator (15) depends on the frequency-domain signals D_0 and c_0. Since D_0 (c_0) can be obtained once d_0 (c_0) is known, and vice versa, the time- and frequency-domain channel estimators (7) and (15) can be directly unified by the extracted DFT matrix **F**0 denoted by (13). Regarding to the optimal design criterion, we have in Section III-A derived (9) for the time-domain training matrix c_0 , while it has been proved in [9] that the optimal frequency domain channel estimator (15) is subject to the following optimal design criterion

$$A_0^H A_0 = N_t L I_{NtL} \quad (16)$$

Using the well-known shift property of DFT, it can be derived that

$$F_{N_p} c_0 = C_0 F_0 = A_0 \quad (17)$$

INTERNATIONAL JOURNAL OF RESEARCH SCIENCE & MANAGEMENT

With the help of (17), the unification of the optimal design criteria (9) and (16) for the time- and frequency-domain channel estimators, respectively, can be revealed by

$$C_0^H C_0 = (F_{N_p}^H A_0)^H F_{N_p}^H A_0 = A_0^H (F_{N_p} F_{N_p}^H) A_0 = A_0^H A_0 \quad (18)$$

It reads clear from (18) that the different design criteria (9) and (16) are essentially equivalent. Therefore, the time- and frequency-domain channel estimators as well as their corresponding optimal design criteria can be unified under the same framework. Channel tracking and data detection in [1].

Performance analysis

This section addresses the performance analysis of the proposed scheme, including the spectral efficiency of proposed TFT-OFDM scheme, the CRLB as well as the computational complexity of the time-frequency joint channel estimation method.

Spectral efficiency:

The spectral efficiency η_0 of the proposed TFT-OFDM MIMO can be expressed in the percentage notation as

$$\eta_0 = \frac{U(N-K)}{U(N+M)+N_p+M-1}, \quad (19)$$

Where $K = G((2d+1)+(N_t-1)(d+1))$

For large-scale 16 × 16 MIMO configuration, i.e., $N_t = N_r = 16$, the number of used pilots in TFT-OFDM is $K = 160$, which is only 3.91% of the total subcarrier number $N = 4096$. Table I clearly indicates that the proposed TFT-OFDM MIMO scheme outperforms its conventional counterparts in spectral efficiency. Since every receive antenna could use the time-frequency joint channel estimation method to distinguish the channels between different transmit antennas and this specific receive antenna, the proposed TFT-OFDM transmission scheme could be used in both scenarios having small (even a single) or large number of receive antennas, and higher spectral efficiency than conventional solutions could be achieved in both cases.

Cramer-rao lower bound:

The CRLB bound is the theoretical bound to evaluate the performance of practical estimation methods [11].

Table1: Spectral Efficiency in MIMO Systems.

Guard interval length	Frequency-domain pilots based MIMO	Time-domain preamble based MIMO	Proposed TFT-OFDM MIMO	MMSE MIMO
M=N/16	75%	80%	88.67%	89.27%

Since the AWGN vector $W_i^{(p)}$ in [1] is subject to the Distribution of $CN(0, \sigma^2 I_G)$, the conditional probability density function (PDF) of $Y_i^{(p)}$ with the given $h_{i,\Gamma}^{(p)}$ is

$$p_{\mathbf{Y}_i^{(p)}|\mathbf{h}_{i,\Gamma}^{(p)}}\left(\mathbf{Y}_i^{(p)};\mathbf{h}_{i,\Gamma}^{(p)}\right) = \frac{1}{(2\pi\sigma^2)^{G/2}} \exp\left\{-\frac{1}{2\sigma^2}\left\|\mathbf{Y}_i^{(p)} - \mathbf{F}_N^{(p)}\mathbf{h}_{i,\Gamma}^{(p)}\right\|^2\right\} \quad (20)$$

The Fisher information matrix [10] of [1] can then be derived as

$$[\mathbf{J}]_{m,n} \triangleq -\mathrm{E}\left\{\frac{\partial^2 \ln\left(p_{\mathbf{Y}_i^{(p)}|\mathbf{h}_{i,\Gamma}^{(p)}}\left(\mathbf{Y}_i^{(p)};\mathbf{h}_{i,\Gamma}^{(p)}\right)\right)}{\partial h_{i,\Gamma,m}^{(p)}\partial h_{i,\Gamma,n}^{(p)}}\right\} = \frac{1}{\sigma^2}\left[\left(\mathbf{F}_N^{(p)}\right)^H\mathbf{F}_N^{(p)}\right]_{m,n}, \quad (21)$$

Where $h_{i,\Gamma,m}^{(p)}$ and $h_{i,\Gamma,n}^{(p)}$ denotes the *m*th and *n*th entry of $h_{i,\Gamma}^{(p)}$, respectively. Finally, according to the vector estimation theory [11], the CRLB of the unbiased estimator $h_{i,\Gamma}^{\wedge(p)}$ is

$$\mathrm{CRLB} = \mathrm{E}\left\{\left\|\widehat{\mathbf{h}}_{i,\Gamma}^{(p)} - \mathbf{h}_{i,\Gamma}^{(p)}\right\|^2\right\} \geq \mathrm{Tr}\left\{\mathbf{J}^{-1}\right\} = \sigma^2\mathrm{Tr}\left\{\left(\left(\mathbf{F}_N^{(p)}\right)^H\mathbf{F}_N^{(p)}\right)^{-1}\right\}. \quad (22)$$

Let $\{\lambda_i\}_{i=0}^{Q}$ being the *Q* eigenvalues of the matrix $(F_N^{(P)})^H F_N^P$, then, we have the following result according to the elementary linear algebra [1]

$$\mathrm{Tr}\left\{\left(\left(\mathbf{F}_N^{(p)}\right)^H\mathbf{F}_N^{(p)}\right)^{-1}\right\} = \sum_{i=1}^{Q}\lambda_i^{-1} = Q\left(\sum_{i=1}^{Q}\lambda_i^{-1}/Q\right) \geq Q\left(Q/\sum_{i=1}^{Q}\lambda_i\right) = \frac{Q^2}{\mathrm{Tr}\left\{\left(\mathbf{F}_N^{(p)}\right)^H\mathbf{F}_N^{(p)}\right\}}, \quad (23)$$

Where the equality holds if and only if $\lambda 1 = \lambda 2 = \cdot\cdot\cdot = \lambda_Q$, which means that the matrix $F_N^{(P)}$ extracted from the standard DFT matrix F_N should have orthogonal columns. Obviously, the $Q \times Q$ matrix $(F_N^{(P)})^H F_N^P$ has identical diagonals equal to *G*, i.e., Tr { $(F_N^{(P)})^H F_N^P$ } = *GQ*, so the CRLB of the proposed time-frequency joint channel estimator becomes

$$\mathrm{CRLB} = \mathrm{E}\left\{\left\|\widehat{\mathbf{h}}_{i,\Gamma}^{(p)} - \mathbf{h}_{i,\Gamma}^{(p)}\right\|^2\right\} = \frac{Q\sigma^2}{G}. \quad (24)$$

Computational complexity:

The computational complexity of the proposed time frequency joint channel tracking scheme can be evaluated in terms of how many multiplications are required in [1].

Simulation result

This section investigates the performance of the proposed TFT-OFDM scheme for large-scale MIMO systems in mobile multipath channels. For performance comparison, the proposed TFT-OFDM scheme for large-scale MIMO systems is compared with its conventional counterparts based on CPOFDM with frequency-domain comb-type pilots [1] and time-domain preamble based iterative channel estimation/data detection scheme in [8], respectively. Note that the spectral efficiency of those three different schemes has been specified in Table I. [1].

INTERNATIONAL JOURNAL OF RESEARCH SCIENCE & MANAGEMENT

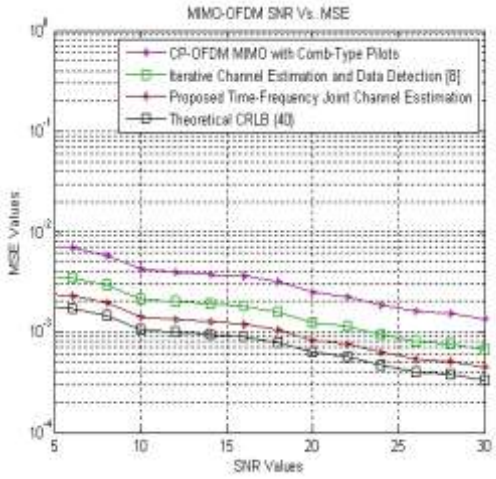

Fig. 1 MSE performance comparison between the proposed time-frequency joint channel estimation method for TFT-OFDM with the conventional schemes.

In Fig. 1 the MSE performance of the proposed time-frequency joint channel estimation for TFTOFDM in large-scale MIMO systems over the Brazil D channel with the receiver velocity of 5 km/h. For comparison, we also include the MSE performance of CP-OFDM with comb-type pilots and the time-domain preamble based iterative channel estimation/data detection scheme for large-scale MIMO systems [8]. In addition, the theoretical CRLB derived in (40) is also plotted as the benchmark for comparison. It is clear that TFT-
OFDM outperforms CP-OFDM and TDSOFDM by about 5 dB when the channel estimation MSE 10^{-2} is considered, and performs 3 dB better than [8]. Also we could observe that the proposed channel estimation performs closely to the theoretical CRLB with a small SNR gap, which is caused by the fact that the "extracted" DFT matrix **F** (*p*) *N* has imperfect but approximate orthogonal columns.

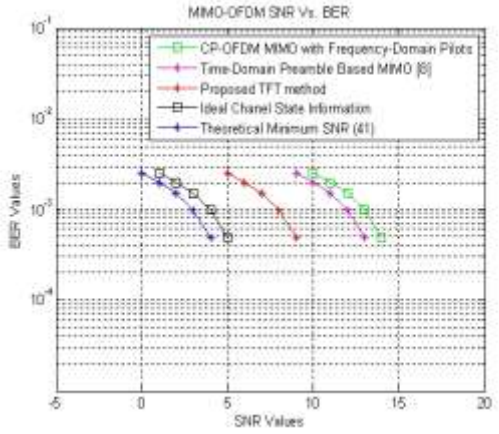

Fig. 2 BER performance comparison between the proposed TFT-OFDM MIMO scheme and its counterparts over the Vehicular B channel with the receiver velocity of 30 km/h.

Conclusions

In this paper, we propose the spectrally efficient TFTOFDM transmission scheme for large-scale MIMO systems to solve the high-dimensional channel estimation issue in mobile environments. Without cyclic prefix, TFT-OFDM has training information in both the time and the frequency domains for every OFDM symbol, and the frequency-domain grouped pilots occupy much fewer subcarriers than that in common CP-OFDM MIMO systems. This is achieved by the time frequency joint channel estimation method, whereby the path delays are firstly acquired by the time-domain received TSs without interference cancellation, then there remains much fewer channel parameters to be estimated by fewer frequency domain pilots. The transmission frame structure composed of one preamble

INTERNATIONAL JOURNAL OF RESEARCH SCIENCE & MANAGEMENT

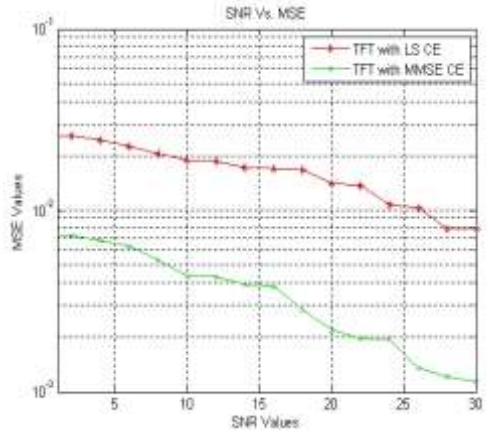

Fig.3 MSE comparison between the least square method and minimum mean square method in TFT OFDM.

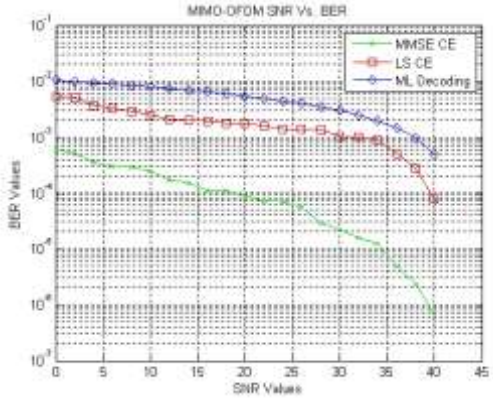

Fig.4 BER comparison between MMSE CE and LS CE in TFT ofdm.

And the subsequent TFT-OFDM symbols could provide efficient channel tracking and data detection in MIMO systems. This paper proves the unification of the time- and frequency-domain channel estimation based on them preamble, and derives CRLB of proposed time-frequency joint channel estimation. Simulation results indicate that the proposed scheme enjoys the BER performance close to the theoretical ergodic capacity. The proposed TFT-OFDM MIMO scheme can be also directly applied in multiple access systems in both the uplink and downlink, and the principle of joint time-frequency processing behind TFT-OFDM can be adapted for other OFDM MIMO systems (including large- and small scale systems) to achieve higher spectral efficiency as well as more reliable performance over severe fading channels.

Acknowledgement

The first author would like to thank Prof. Feifei Gao for his valuable support for this paper. The authors would like to thank the Guest Editor and the anonymous reviewers for their helpful comments and suggestions to improve the quality of this manuscript. Appendix proof of (15) and (16) in [11]

References

1. L. Dai, Z. Wang, and Z. Yang, "spectrally efficient time-frequency training OFDM for Mobile large scale MIMO systems", IEEE Commun. Mag., vol. 31, no. 2, pp. 251–262, Feb. 2013.
2. L. Dai, Z. Wang, and Z. Yang, "Next-generation digital television terrestrial broadcasting systems: Key technologies and research trends," IEEE Commun. Mag., vol. 50, no. 6, pp. 150–158, Jun. 2012.
3. IEEE Standard for Information Technology-Part 11: Wireless LAN Medium Access Control (MAC) and Physical Layer (PHY) Specifications Amendment: Enhancements for Higher Throughput. IEEE Standard802.11n-2009, Oct. 2009.

INTERNATIONAL JOURNAL OF RESEARCH SCIENCE & MANAGEMENT

4. IEEE Standard for Local and Metropolitan Area Networks Part 16: Air Interface for Broadband Wireless Access Systems. IEEE Standard802.16-2009, May 2009.
5. 3rd Generation Partnership Project; Technical Specification Group Radio Access Network; Evolved Universal Terrestrial Radio Access (EUTRA) and Evolved Universal Terrestrial Radio Access Network (EUTRAN); Overall description; Stage 2 (Release 8). 3GPP TS 36.300, V8.5.0, May 2008.
6. F. Rusek, D. Persson, B. K. Lau, E. G. Larsson, O. Edfors, F. Tufvesson, and T. L. Marzetta, "Scaling up MIMO: Opportunities and challenges with very large arrays," IEEE Signal Process. Mag., 2012. (in press).
7. M. Matthaiou, N. Chatzidiamantis, and G. Karagiannidis, "A new lower bound on the ergodic capacity of distributed MIMO systems," IEEESignal Process. Lett. vol. 18, no. 4, pp. 227–230, Apr. 2011.
8. S. K. Mohammed, A. Zaki, A. Chockalingam, and B. S. Rajan, "Highratespace–time coded large-MIMO systems: Low-complexity detection and channel estimation," IEEE J. Sel. Topics Signal Process., vol. 3,no. 6, pp. 958–974, Dec. 2009.
9. H. Taoka and K. Higuchi, "Experiments on peak spectral efficiency of 50 bps/Hz with 12-by-12 MIMO multiplexing for future broadband packet radio access," in 4th IEEE International Symposium on Communications, Control and Signal Processing (ISCCSP'10), 2010, pp. 1–6.
10. G. Breit and et al., 802.11 ac Channel Modeling. IEEE 802.11 TGac: Very High Throughput below 6GHz Group doc. 09/0088, Jan. 2009.
11. S. M. Kay, Fundamentals of Statistical Signal Processing, Volume I: Estimation Theory. New Jersey, USA: Prentice-Hall, 1993